



Alteration of Absorption Spectra with Variations in Gold Nanocage Geometries: A Numerical Study

Fatema Alali^{a*}, Abdullah AlKharif^b

^{a,b} *Electronic Engineering Dept., College of Technological Studies, Public Authority for Applied Education and Training, Kuwait City 13092, Kuwait*

^a*Email: fa.alali@paaet.edu.kw*, ^b*Email: am.alkharif@paaet.edu.kw*

Abstract

Nanocages are one of the vastly exploited nanoparticles in photothermal therapy and drug delivery via exciting their localized surface plasmon resonance (LSPR). LSPR depends on the nanoparticle shape, size, and orientation. Any alteration in the particle's geometry can significantly shift its LSPR and can be accompanied by a drop in absorption power. This is a drawback in photothermal-based applications where field intensity and resonance wavelength accuracy determine the treatment efficiency. Nanocages differ from typical solid geometries because they are porous along all the orthogonal axes. Thus, for an optimized response, additional consideration must be given to the effect of their dimensions on the resonance. We examine the absorption of nanocages with various geometric features using full-wave electromagnetic analysis via the commercial software COMSOL. Furthermore, we investigate the spectrum variations of nanocages with multiple aspect ratios and detect their energy distribution in several peaks and the impact of truncated edges on the spectrum. Moreover, for colloidal nanoparticles, we demonstrate the absorption polarization sensitivity of nanocages at random orientations, where particle orientations significantly affect their absorption spectrum. Our study presents a beneficial view regarding geometry effects on metallic nanocages LSPR, which can be utilized for optimizing photothermal response in different biomedical applications.

Keywords: nanocage; photothermal therapy; nanoparticle; optics; photothermal energy; plasmonics; absorption spectrum.

Received: 5/21/2023

Accepted: 6/28/2023

Published: 7/8/2023

* Corresponding author.

1. Introduction

One of the most interesting properties of metallic nanoparticles is localized surface plasmon resonance (LSPR). Due to the confinement effect, illuminated particles with dimensions less than the light wavelength (1–100 nm) experience new phenomena than those of bulk materials. When a nanoparticle is irradiated with a specific wavelength (λ_{LSPR}), conducting electrons vibrate coherently within the limited area of the nanoparticle. During their relaxation period (0.1–1 ns), excited electrons dissipate thermal energy into their surroundings and generate a highly localized electric field accompanied by a resonance peak in the absorption spectrum of the nanoparticle (1,9). The size and shape of nanoparticles significantly impact the LSPR, and these geometrical factors result in λ_{LSPR} ranging from the ultraviolet (UV) to the near-infrared (NIR) region. For biomedical applications, two NIR windows have been defined: the commonly known NIR-I (700–1000 nm) and the new NIR-II (1000–1400 nm), which requires lower laser intensity than NIR-I, making it safer for skin tissue penetration [10]. Photothermal therapy exploits the high absorption accompanied by LSPR, where photon energy is converted to relatively intense heat surrounding the excited nanoparticle. The excitation is achieved from a pulsed laser within NIR frequency to ensure tissue penetration. Laser energy is regulated to produce a field intense enough to destroy harmful cells with minimal damage to healthy tissues and without deforming the nanoparticle shape from immoderate heating (11,14). Targeting and damaging cancer cells via plasmonic nanoparticle aggregation is one major photothermal-based approach in medical fields (15,16). This approach is highly recognized due to its low side effects and minimal invasiveness to healthy tissues [17]. Moreover, the photothermal effect enhances the cell's permeability, enabling more particle accumulation in the tumor. Thus, reducing the required dose for treatment [16].

Among various metallic nanoparticles, gold is the most suitable for biomedical applications due to its advantages in photothermal therapy implementations, such as chemical stability and low toxicity (15,16,18,20). Different geometries of gold nanoparticles have been fabricated and studied for photothermal applications, including nanospheres, nanoshells, nanorods, nanotori (nanorings), and nanocages (21,24).

Gold nanocages represent new and recent development in nanoparticle synthesis that is particularly suited for photothermal therapeutic applications (16,7,24,25). Numerical analyses have been conducted to explore the optical response of gold nanocages [24]. One significant advantage of this design is that it is easily produced in large quantities using bottom-up approaches [26]. In comparison to other nanostructures, nanocages are distinguished by their porosity. Considering their porous nature, gold nanocages can be distinguished from nanoparticles of comparable size by examining transmission electron microscopy (TEM) images and employing nanocage-based biomarkers. Nanocages are ideally suited for drug encapsulation and optically controlled photothermal drug delivery because of their porous characteristics (19,24). It is interesting and worthwhile to mention that the superiority of nanocages for drug delivery is not limited to metallic structures but expands to molecular structures. It has been reported that boron nitride-based nanocage, $\text{B}_{12}\text{N}_{12}$, shows an increase in drug adsorption when infused with metallic atoms such as platinum (Pt)(27,28) or gold (Au) [29]. This metallic atom addition modifies the nanocarrier's molecular structure and changes the dipole moment and energy level gaps of $\text{B}_{12}\text{N}_{12}$ enhancing drug absorption. This paper examines the optical properties associated with the LSPR excitation of gold nanocages as metallic structures.

2. Computational Methods

We employ 3D time-harmonic full-wave field theory to conduct numerical simulations using the COMSOL Wave Optics module based on the finite element method (www.comsol.com). The incident field, created by a surface current (not shown) in the xy -plane at the top of the computational domain, is directed at the nanocage (Figure. 1), which is located at the domain's origin (Figure. 2a). This produces a TEM plane wave with the electric field polarized in the x -direction and the wave propagating downwards along the z -axis as indicated by the k vector.

As detailed in our prior work(22,25), a perfect electric conductor and perfect magnetic conductor are applied on the boundaries perpendicular to the electric and magnetic fields, respectively. Perfectly matched layer conditions have been defined at the top and bottom of the domain to reduce the backscattering fields due to metallic particle excitation. We solve the time-harmonic electric field equation:

$$\nabla \times (\mu_r^{-1} \nabla \times \vec{E}) - k_0^2 \left(\epsilon_r - j \frac{\sigma}{\omega \epsilon_0} \right) \vec{E} = 0 \quad (1)$$

Where E is the electric field, μ_r and ϵ_r are the relative permeability and permittivity of the media, respectively. For a given gold nanocage, we use $\mu_r = 1$. The permittivity ϵ_r is predicted using an analytical formula based on a Drude–Lorentz model. The parameters for this equation are available in the scientific literature [30,31]. We mimic the particle's surrounding conditions for biomedical applications by setting the nonabsorbing water refractive index for the computational domain volume as $n = 1.33$.

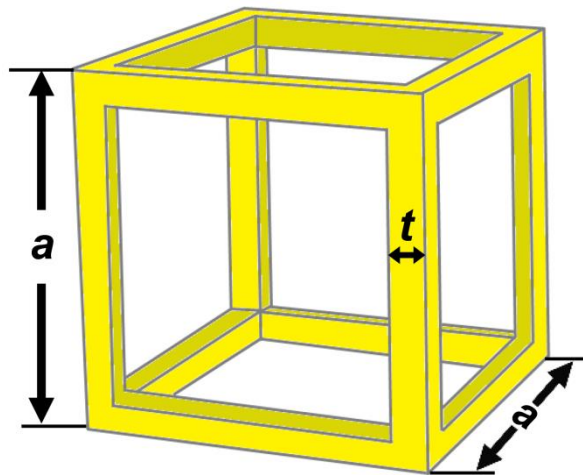


Figure 1: Nanocage structure and characteristic dimensions.

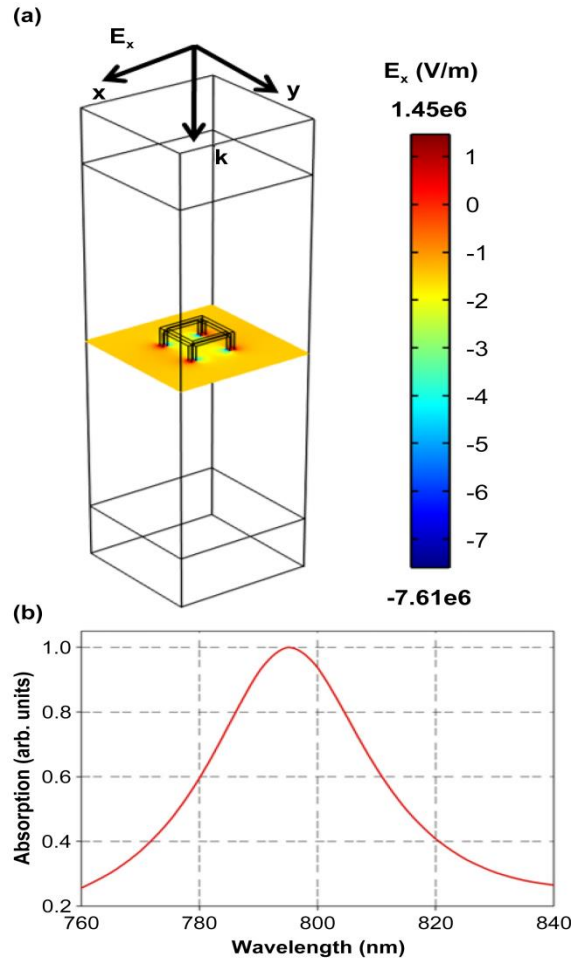


Figure 2: Photonic analysis of a gold nanocage ($a = 50$ nm and $t = 5$ nm) with parallel alignment to the incident polarization: (a) computational domain and plot of the linearly x-axis polarized electric field (E_x) through a cross section of the domain; (b) absorbed power vs. wavelength at parallel orientation.

3. Results and Discussion

We investigated the behavior of a cubic nanocage with the dimensions shown in Figure. 1. Conventional nanostructure resonance can be generally modified by adjusting their aspect ratio, such as length/width for the rods. These characteristics are determined by the solid geometry dimensions. Regarding the proposed nanocages' the aspect ratio is defined as the outer edge length (a)/thickness (t). Figure. 2a presents the computational domain for the nanocage geometry. As a function of the wavelength for $\lambda = 760\text{--}840$ nm, we performed a parametric analysis of the power absorbed by the nanocage with a length of 50 nm and a thickness of 5 nm, and plasmon resonance occurred at 795 nm (Figure. 2b). It is well known that the fixed aspect ratios do not induce frequency shifts in the LSPR [21-24]. The calculations indicate that for a given constant a/t ratio, there is no variation in the LSPR spectrum (Figure. 3). The peak height is proportional to the nanocage size: the larger the nanocage, the higher the peak. Nanocage's LSPR is significantly affected by its shape and size. It has been demonstrated that for a given t and a , peak height will vary (24,32). Our results indicate that nanocages with a fixed $t = 5$ nm and $a > 40$ nm exhibit multiple resonance peaks in the optical range 600–1200 nm (Figure. 4a).

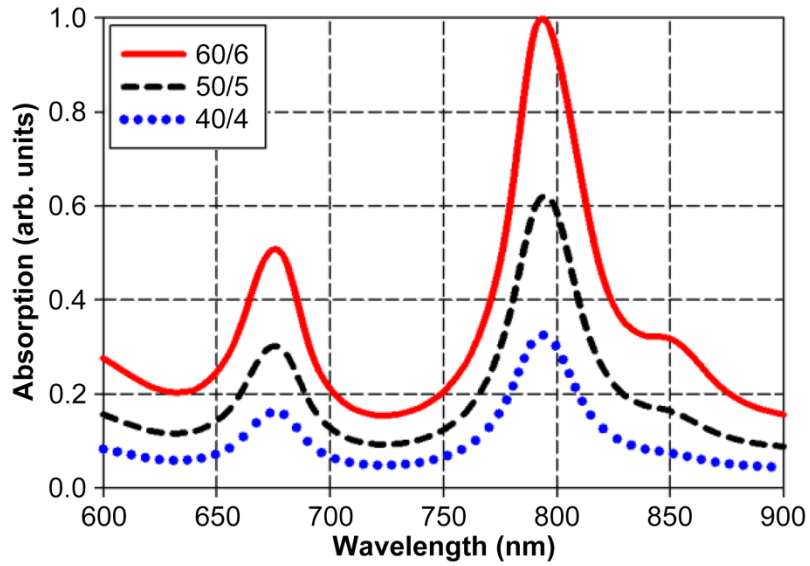


Figure 3: Absorption spectra of nanocages with different sizes and a fixed aspect ratio $X = a/t = 10$.

Thus, as the aspect ratio increases, their resonance red shifts. This aspect ratio-dependent shift agrees with the previously reported results [33].

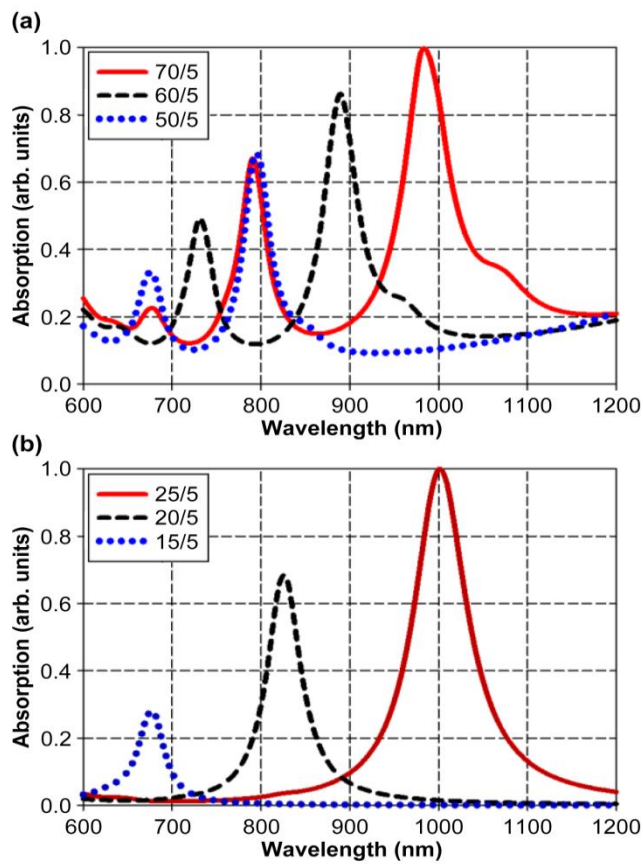


Figure 4: Absorption spectra for nanocages with a fixed thickness and with outer edges being (a) larger and (b) smaller than 40 nm. Resonance peaks red-shifted with the increasing aspect ratio.

As displayed in Figure. 4b, the energy is concentrated in a single resonance peak for nanocages with a size of less than 40 nm. This explains the significant absorption recorded for nanocages smaller than 45 nm in a previous study [32]. As shown in Figure. 4, the increased aspect ratio shifts LSPR toward NIR-II. However, the frame size needs to be taken into consideration because, unlike the single concentrated peak of smaller frames, larger frames split energy among multiple peaks, resulting in lower resonance intensity in the NIR.

Another factor that can cause an additional shift in nanocages LSPR is the truncated corners that occur during the nanocage fabrication. In Figure. 5, truncated corners in dashed red lines are compared to the non-truncated corners in dotted blue lines for two nanocages with aspect ratios of 50/5 and 40/5. Compared to non-truncated nanocages, this technique resulted in truncated corners (26,34), producing a greater LSPR shift. In addition to LSPR redshift, these findings reveal that truncated corners divide absorption energy into more peaks resulting in resonance peaks with lower absorption power than non-truncated ones. Finally, the effect of random orientations on the resonance absorption of a nanocage was considered. Nanocages were used as colloidal nanoparticles in biomedical applications, including photothermal cancer therapy. The absorption efficiency of different colloidal nanoparticles varies depending on the particle orientation [23]. As a result of the symmetry of the nanocage geometry, its absorption is believed to be resistant to random orientations, like that of a nanosphere. In other words, resonance absorption of a nanocage has weak dependence on its orientation. This is consistent with the results obtained in a previous study [24].

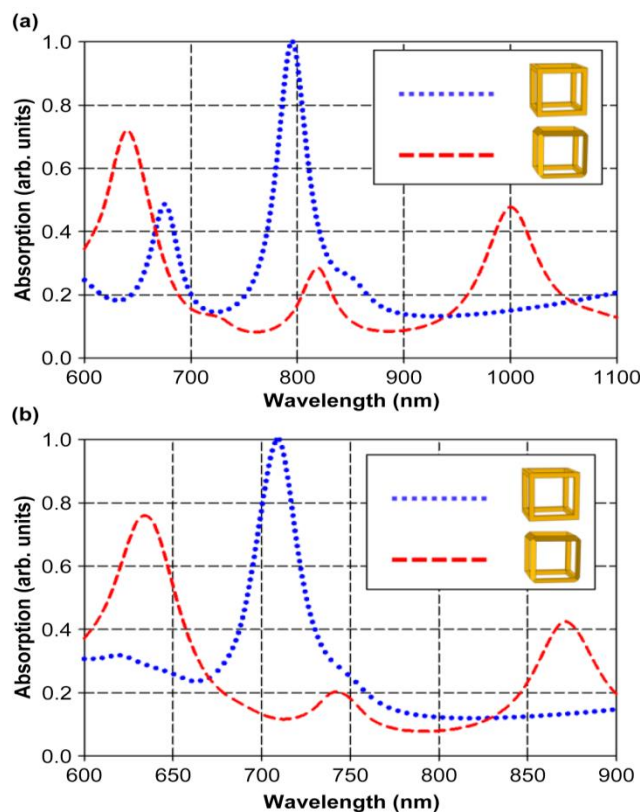


Figure 5: A comparison in absorption spectrum between truncated (red dashed lines) and non-truncated (dotted blue line) nanocages with an aspect ratio of (a) 50/5 and (b) 40/5. The truncated corners divide energy into more peaks that spread along a broader spectrum range.

As anticipated, Figure 6 demonstrates that nanocage absorption has low sensitivity to the polarization direction. This can be attributed to the nanocage being composed of orthogonal nanorods.

Nanorods have a high absorption for polarization along their major axis (length) which corresponds to the angles between $40^\circ < \theta < 90^\circ$ and $0^\circ < \phi < 40^\circ$. Due to the geometry of nanocages, a set of rods will always fall within this range of angles for any given orientation [23].

However, this low polarization sensitivity of randomly oriented colloidal nanoparticles is important in biomedical applications.

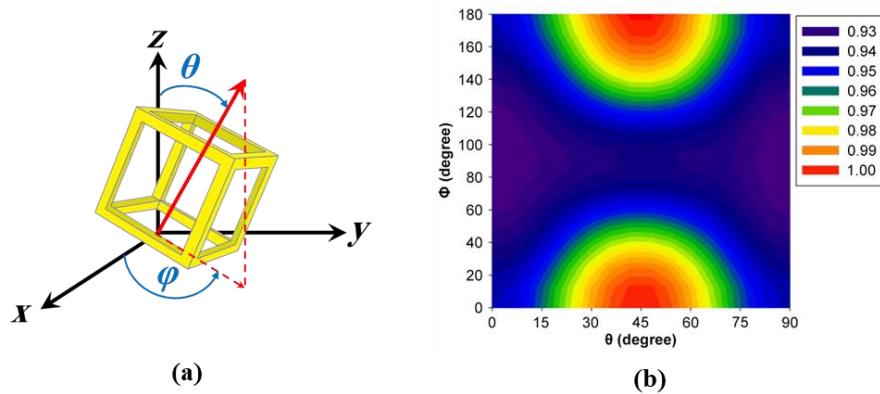


Figure 6: (a) Nanocage orientation characterized using spherical coordinate angles θ and ϕ . (b) Nanocage absorption at a fixed LSPR wavelength as a function of orientation (θ and ϕ) at $\lambda = 795$ nm ($a = 50$ nm, $t = 5$ nm).

4. Conclusions

We employed computational electromagnetic analysis to study the impact of geometrical variation on the LSPR of nanocages. We demonstrated that absorption energy splits into multiple resonance peaks in nanocages with a fixed t and a variable $a > 40$ nm. While for $a < 40$ nm, energy is concentrated in a single peak resulting in greater absorption energy at a resonance wavelength. Furthermore, we compared the spectra of truncated and non-truncated nanocages, where the latter distributes absorption energy into more peaks, resulting in a higher LSPR redshift and a lower overall resonance peak. Though increasing aspect ratio red shifts LSPR for nanocages, our results show that this shift is limited to the NIR-I upper bound ($\lambda_{\text{LSPR}} \sim 1000$ nm). For biomedical applications, it is more effective to have LSPR beyond NIR-II lower bound ($\lambda_{\text{LSPR}} > 1000$ nm). Finally, we have demonstrated that nanocages with random orientations resist absorption polarization, a significant advantage for colloidal particles in biomedical applications. Currently, we are investigating other shapes of porous nanoparticles for LSPR redshift toward NIR-II (1000–1400 nm), and we'll report our results in future work.

5. Disclosures

The authors have no conflicts to disclose.

Acknowledgments

The authors would like to thank Enago (www.enago.com) for the English language review.

Data availability

All data are available within the article.

References

- [1] K. L. Kelly et al., "The optical properties of metal nanoparticles: the influence of size, shape, and dielectric environment," *J. Phys. Chem. B* **107**, 668 (2003).
- [2] S. Link and M.A. El-Sayed, "Shape and size dependence of radiative, non-radiative and photothermal properties of gold nanocrystals," *Int. Rev. Phys. Chem.* **19**, 409 (2000).
- [3] L. M. Liz-Marzán, "Tailoring surface plasmons through the morphology and assembly of metal nanoparticles," *Langmuir* **22**, 32 (2006).
- [4] M. A. El-Sayed, "Small is different: shape-, size-, and composition-dependent properties of some colloidal semiconductor nanocrystals," *Acc. Chem. Res.* **37**, 326 (2004).
- [5] X. Ma et al., "Electronic and optical properties of strained noble metals: implications for applications based on LSPR," *Nano Energy* **53**, 932 (2018).
- [6] W. He et al., "Significant temperature effect on the LSPR properties of noble metal nanoparticles," *J. Opt.* **51**, 142 (2022).
- [7] C. C. Jian, J. Zhang, and X. Ma, "Cu–Ag alloy for engineering properties and applications based on the LSPR of metal nanoparticles," *RSC Adv.* **10**, 13277 (2020).
- [8] M. L. Brongersma, N. J. Halas, and P. Nordlander, "Plasmon-induced hot carrier science and technology," *Nat Nanotechnol.* **10**, 25 (2015).
- [9] M. Kim et al., "Hot-electron-mediated photochemical reactions: principles, recent advances, and challenges," *Adv. Opt. Mater.* **5**, 1700004 (2017).
- [10] P. Vijayaraghavan et al., "Complete destruction of deep-tissue buried tumors via combination of gene silencing and gold nanochinus-mediated photodynamic therapy," *Biomaterials* **62**, 13 (2015).
- [11] C. M. Pitsillides et al., "Selective cell targeting with light-absorbing microparticles and nanoparticles," *Biophys. J.* **84**, 4023 (2003).
- [12] M. Kim et al., "Plasmonic photothermal nanoparticles for biomedical applications," *Adv. Sci.* **6**, 1900471 (2019).
- [13] D. Jaque et al., "Nanoparticles for photothermal therapies," *Nanoscale* **6**, 9494 (2014).
- [14] J. V. Frangioni, "In vivo near-infrared fluorescence imaging," *Curr. Opin. Chem. Biol.* **7**, 626 (2003).
- [15] J. B. Vines et al., "Gold nanoparticles for photothermal cancer therapy," *Front. Chem.* **7**, 167 (2019).
- [16] R.S. Riley and E. S. Day, "Gold nanoparticle-mediated photothermal therapy: applications and opportunities for multimodal cancer treatment," *Wiley Interdiscip. Rev. Nanomed. Nanobiotechnol.* **9**, e1449 (2017).
- [17] A. Kumar, S. Kim, and J. M. Nam, "Plasmonically engineered nanoprobe for biomedical

- applications,” *J. Am. Chem. Soc.* **138**, 14509 (2016).
- [18] X. Cheng et al., “Light-triggered assembly of gold nanoparticles for photothermal therapy and photoacoustic imaging of tumors in vivo,” *Adv. Mater.* **29**, 1604894 (2017).
- [19] N. Khlebtsov et al., “Analytical and theranostic applications of gold nanoparticles and multifunctional nanocomposites,” *Theranostics* **3**, 167 (2013).
- [20] D. A. Giljohann et al., “Gold nanoparticles for biology and medicine,” *Angew. Chem. Int. Ed. Engl.* **49**, 3280 (2010).
- [21] G. Baffou and R. Quidant, “Thermo-plasmonics: using metallic nanostructures as nano-sources of heat,” *Laser & Photonics Reviews Laser Photon Rev.* **7**, 171 (2013).
- [22] F. Alali et al., “Hybridization of plasmon modes in multishell bimetallic nanoparticles: a numerical study,” *J. Nanophoton.* **14**, 036007 (2020).
- [23] F. Alali et al., “Photonic and thermofluidic analysis of colloidal plasmonic nanorings and nanotori for pulsed-laser photothermal applications,” *J. Phys. Chem. C* **117**, 20178 (2013).
- [24] I. H. Karampelas, K. Liu, F. Alali, and E. P. Furlani, “Plasmonic nanoframes for photothermal energy conversion,” *J. Phys. Chem. C* **120**, 7256 (2016).
- [25] M. Laudon and B. F. Romanowicz, “Numerical analysis of laser induced photothermal effects using colloidal plasmonic nanostructures,” *Nano Science and Technology Institute., TechConnect Briefs* **1**, 312 (2014).
- [26] S. E. Skrabalak et al., “Gold nanocages: Synthesis, properties, and applications,” *Acc. Chem. Res.* **41**, 1587 (2008).
- [27] Y. Cao et al., “Investigations of adsorption behavior and anti-cancer activity of curcumin on pure and platinum-functionalized B12N12 nanocages,” *J. Mol. Liq.* **334**, 116516 (2021).
- [28] Y. Li et al., “Dense heterointerfaces and unsaturated coordination synergistically accelerate electrocatalysis in Pt/Pt5P2 porous nanocages,” *Adv. Funct. Mater.* **32**, 2205985 (2022).
- [29] N. Abdolahi et al., “Gold decorated B12N12 nanocluster as an effective sulfasalazine drug carrier: a theoretical investigation,” *Physica E: Low Dimens. Syst. Nanostruct.* **124**, 114296 (2020).
- [30] P. B. Johnson and R. W. Christy, “Optical constants of the noble metals,” *Phys. Rev. B* **6**, 4370 (1972).
- [31] P. G. Etchegoin, E. C. le Ru, and M. Meyer, “An analytic model for the optical properties of gold,” *J. Chem. Phys.* **125**, 164705 (2006).
- [32] S. E. Skrabalak et al., “Gold nanocages for biomedical applications,” *Adv. Mater.* **19**, 3177 (2007).
- [33] X. Wang, A. Ruditskiy, and Y. Xia, “Rational design and synthesis of noble-metal nanoframes for catalytic and photonic applications,” *Natl. Sci. Rev.* **3**, 520 (2016).
- [34] J. Chen et al., “Facile synthesis of gold–silver nanocages with controllable pores on the surface,” *J. Am. Chem. Soc.* **128**, 14776 (2006).

Fatema Alali received her BE degree in electrical engineering from the Kuwait University in 2000, and her MS and PhD degrees in electrical engineering from University at Buffalo, New York, in 2004 and 2013, respectively. In 2002, she joined as a faculty in the Department of Electronic Engineering in the Public Authority for Applied Education and Training (PAAET), Kuwait. Currently, she is an assistant professor in PAAET, and her research focuses on nanophotonics.

Abdullah Alkharif received his BS degree in Computer Engineering from the California State University, Long Beach. In 2005, he joined the Public Authority for Applied Education and Training (PAAET), Kuwait, as a faculty of training in the Department of Electronic Engineering. Currently, He is a Training Specialist in College of Technological Studies, and his research focuses on embedded systems, IoT system development.